Platinum-Nanoparticle-Modified TiO_2 Nanowires with Enhanced Photocatalytic Property

Chengxiang Wang, Longwei Yin,* Luyuan Zhang, Ningning Liu, Ning Lun, and Yongxin Qi

Key Laboratory for Liquid–Solid Structural Evolution & Processing of Materials, Ministry of Education, School of Materials Science & Engineering, Shandong University, Jinan 250061, P.R. China

ABSTRACT Highly crystalline Pt nanoparticles with an average diameter of 5 nm were homogeneously modified on the surfaces of TiO_2 nanowires (Pt-TiO_2 NWs) by a simple hydrothermal and chemical reduction route. Photodegradation of methylene blue (MB) in the presence of Pt-TiO_2 NWs indicates that the photocatalytic activity of TiO_2 NWs can be greatly enhanced by Pt nanoparticle modification. The physical chemistry process and photocatalytic mechanism for Pt-TiO_2 NWs hybrids degrading MB were investigated and analyzed. The Pt attached on TiO_2 nanowires induces formation of a Schottky barrier between TiO_2 and Pt naonoparticles, leading to a fast transport of photogenerated electrons to Pt particles. Furthermore, Pt incoporation on TiO_2 surface can accelerate the transfer of electrons to dissolved oxygen molecules. Besides enhancing the electron–hole separation and charge transfer to dissolved oxygen, Pt may also serve as an effective catalyst in the oxidation of MB. However, a high Pt loading value does not mean a high photocatalytic activity. Higher content loaded Pt nanoparticles can absorb more incident photons which do not contribute to the photocatalytic efficiency. The highest photocatalytic activity for the Pt-TiO_2 nanohybrids on MB can be obtained at 1 at % Pt loading.

KEYWORDS: TiO_2 NWs • platinum • hybrids • modification • photocatalytic activity

INTRODUCTION

Photocatalytic decomposition of organic contaminants is one of the promising techniques for the treatment of wastewater. Because of their high photocatalytic activity, stability, and nontoxicity, the TiO_2 nanomaterials have especially attracted increased attention in the research and application of photocatalysis (1–5). A variety of TiO_2 nanomaterials, such as nanotubes (6), nanowires (7, 8), nanoparticles (9), nanocrystal films (10), nanotube arrays (11), etc., have been reported. TiO_2 nanowires and nanotubes can be served not only as the photocatalysts but also as good substrates for the enhancement of photocatalytic activity by modification.

However, the overall quantum efficiency of pure TiO_2 is relatively low. It is decided by the competition between charge-carrier recombination, trapping, and interfacial charge transfer (12). The trapping of the photogenerated electrons on the surface is very fast. However, photocatalytic reduction rate is much slower than that of oxidation process (12, 13). If there are no appropriate acceptors on the surface, the trapped electrons will recombine with the holes quickly. Noble metal deposition seems to provide a way to solve this problem. Emilio et al. (14) observed an increase in the lifetime of electrons by Pt modification on the TiO_2 surface, due to a better separation of charge carriers caused by the schottky barrier between Pt and TiO_2. As expected, this will help to increase the photocatalytic efficiency of TiO_2 (10, 15, 16). Though the effect of Pt modification is obvious, the mechanism is still not very clear. Pt is an effective catalyst in process of hydrogenation, dehydrogenation and oxidation in thermal catalysis, which may also prove beneficial during photocatalysis (10). However, this has been ignored by many authors in the investigation of photocatalytic reactions of Pt modified TiO_2 materials.

In the present work, the Pt-TiO_2 NWs hybrids with Pt nanoparticles homogeneously deposited on the surface of TiO_2 NWs were fabricated by a simple hydrothermal and chemical reduction method. The influence of Pt loading values on photocatalytic efficiency was investigated. Photodegradation methylene blue (MB) illuminated under UV light suggests that the photocatalytic activity of TiO_2 NWs can be greatly enhanced by Pt nanoparticle modification. The highest photocatalytic activity on MB for the Pt-TiO_2 nanohybrids can be obtained at 1 at % Pt loading. The physical chemistry process and mechanism of photocatalysis of Pt-TiO_2 nanohybrids were discussed and analyzed.

EXPERIMENTAL SECTION

Preparation of TiO_2 NWs. The TiO_2 NWs were prepared according to the following process (6). 0.2 g TiO_2 powder was added to 20 mL of 8 M NaOH solutions and stirred for 2 min. Then the mixture was transferred to Teflon-lined autoclave and kept at 240 °C for 5 h. After being cooled to room temperature, the white products were collected by vacuum filter. The products were washed with deioned water until there were no residual ions. After being dried at 60 °C, the products were calcined at 500 °C for 3 h.

Preparation of Pt-TiO_2 NWs Composites. The deposition of Pt on TiO_2 was carried out in a chemical reduction method. 0.08 g (0.001 mol) as-prepared TiO_2 powder was mixed with 50 mL glycol. After sonication for 20 min, the mixture was

* Author to whom correspondence should be addressed. Phone: +86-531-88396970. E-mail: yinlw@sdu.edu.cn.

Received for review September 4, 2010 and accepted October 7, 2010

DOI: 10.1021/am100834x

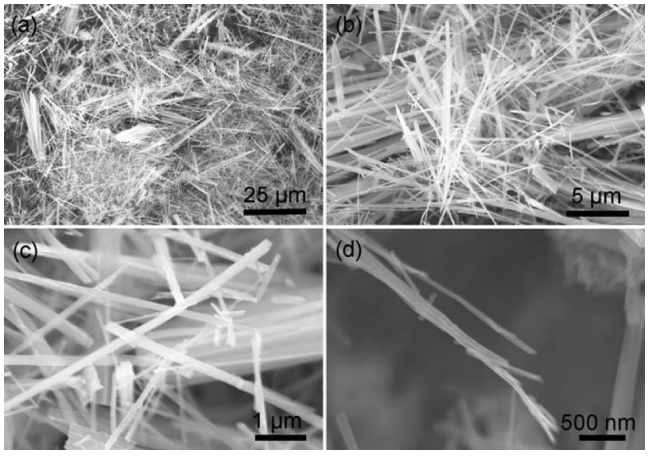

FIGURE 1. SEM images of the 1 at % Pt-TiO_2 sample with different magnifications.

transferred to a three-neck flask. When the mixture was heated to 160 °C under magnetic stirring, a certain volume of 0.05 M H_2PtCl_6 solution was injected rapidly. After keeping at 160 °C for 15 min, the black precipitation was centrifuged and kept at 60 °C for 5 h in the air. The volumes of H_2PtCl_6 solution were 0.1, 0.2, and 0.4 mL, respectively. There was no loss of Pt in the preparation process. So, the Pt loading content was 0.5, 1, and 2 at %, respectively.

Structure Characterization. Samples of the as-prepared products were characterized by X-ray powder diffraction (XRD) with a Rigaku D/max-kA diffractometer with CuKa radiation (60 kV, 40 mA). The morphologies of the products were analyzed using SU-70 field emission scanning electron microscopy (FE-SEM). The structures of the products were analyzed using a high-resolution transmission electron microscope (HRTEM) of Tecnai 20U-Twin at an acceleration voltage of 200 kV.

Photodegradation of MB. Photodegradation of MB was carried out in a photochemical reactor. The UV spectrum and concentration of MB were obtained in TU-1901 double-beam UV−visible spectrophotometer. FTIR spectrum was obtained on Bruker Tensor27 FTIR spectrometer using KBr pellets. The concentration of MB was 20 mg/L. 12.5 mg photocatalyst was added into 50 mL MB solutions in each group. The solutions were fetched every 20 min. The total reaction time was 100 min.

RESULTS AND DISCUSSIONS

Figure 1 shows SEM images of the 1 at % Pt-TiO_2 sample. The sample exhibits uniform nanowires with the diameter of 100−200 nm. There are also some bundles of nanowires, which exhibit large diameters. However, there are no obvious indications to prove the deposition of Pt on the surface of nanowires. This is because the Pt nanoparticles are too small to be detected.

The microstructure of the 1 at % Pt-TiO_2 sample was further investigated by TEM. Images a and b in Figure 2 show the uniform TiO_2 NWs, images c and d in Figure 2 show TEM image of single TiO_2 NWs. It can be clearly observed that Pt nanoparticles were deposited on the surface of the TiO_2 NWs from images c and d in Figure 2. The Pt nanoparticles are very fine, with the average size of 5 nm. They covered the surfaces of TiO_2 nanowires uniformly.

High-resolution transmission electron microscopy (HRTEM) was used to investigate the crystal structure of the Pt-TiO_2 NWs hybrids as shown in figure 3. The *d*-spacing of

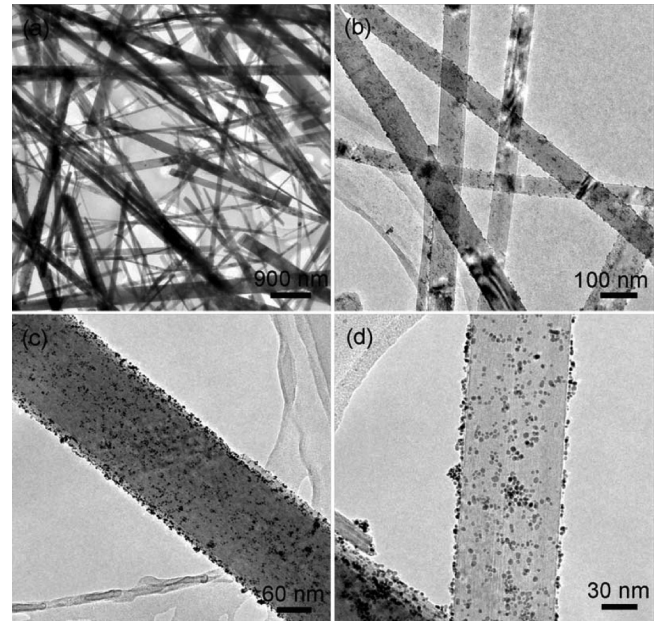

FIGURE 2. TEM images of 1 at % Pt-TiO_2 sample with different magnification.

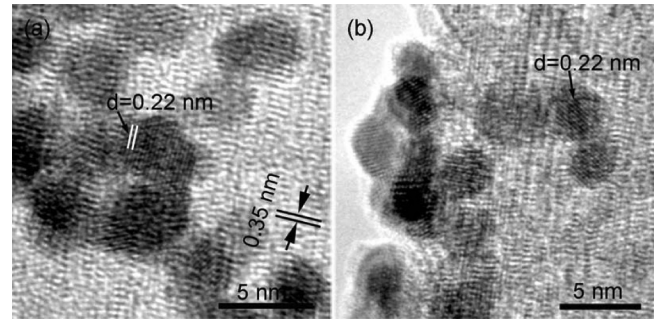

FIGURE 3. HRTEM images of 1 at % Pt-TiO_2 sample. The *d*-spacing of 0.22 nm corresponds well with that of Pt (111) planes. The *d*-spacing of 0.35 nm corresponds well with that of (101) plane of anatase TiO_2.

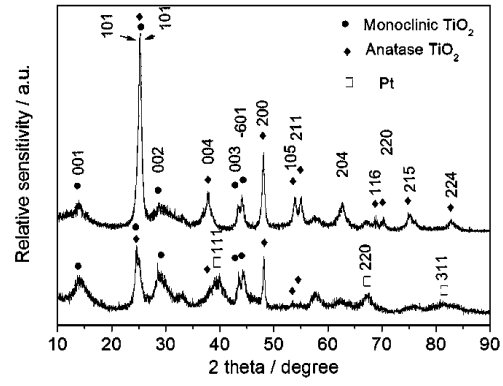

FIGURE 4. XRD patterns of samples (a) 1 at % Pt-TiO_2, (b) pure TiO_2 NWs.

0.22 nm in figure 3 corresponds well with that of Pt (111) planes. The exposure facets of Pt nanoparticles were mainly (111) planes. The *d*-spacing of 0.35 nm corresponds well with that of (101) plane of anatase TiO_2.

Figure 4 shows the XRD patterns of TiO_2 NWs with or without Pt nanoparticle modification. The TiO_2 NWs are mainly composed of anatase (JCPDS No. 21−1272) and

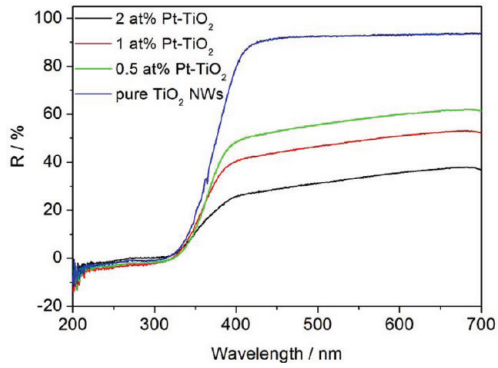

FIGURE 5. Diffuse reflectance spectroscopies of samples with different Pt/TiO_2 ratios.

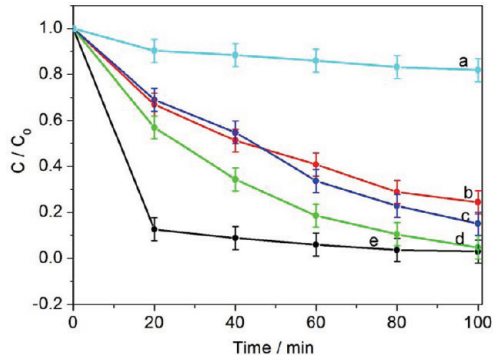

FIGURE 6. Time-depended photodegradation of MB (20 mg/L, 50 mL) under the illumination of UV light (a) without photocatalysts, (b) 2 at% Pt-TiO_2, (c) 0.5 at% Pt-TiO_2, (d) 1 at% Pt-TiO_2, and (e) pure TiO_2 NWs. All the photocatalysts were used without prior adsorptions of MB.

monoclinic (JCPDS No. 46−1237) phases. High diffraction peaks indicate that TiO_2 NWs are crystalline which is very important for photocatalysts. After modified by Pt (JCPDS No. 65−2868) nanoparticles, the diffraction peaks of Pt (111), (220), and (311) crystal plane can be observed in Figure 1a. Broadening of Pt peaks indicates that the Pt nanoparticles are very small.

For photocatalysis application, UV−visible light absorption properties are very important. Figure 5 shows the diffuse reflectance spectrum (DRS) of different samples. Pure TiO_2 NWs reflect about 95% of the visible light and absorb almost all ultraviolet light. Pt-TiO_2 NWs show some differences with pure TiO_2 NWs. In fact, highly dispersed platinum nanoparticles can absorb nearly all the incident light (17). This means that in all the wavelength range of 200−700 nm, the reflectance of Pt-TiO_2 NWs is lower than that of pure TiO_2 NWs. As shown in Figure 5, in the visible region, the reflectance of Pt-TiO_2 NWs is obviously lower than that of pure TiO_2 NWs. However, in the ultraviolet region, it is not obvious because of the very high adsorption of ultraviolet light for pure TiO_2 NWs. With the Pt loading value increasing, the reflectance of Pt-TiO_2 NWs decreases but the shape of the spectra is similar with that of pure TiO_2 NWs.

The time-dependent photodegradation of MB was used to examine the influence of Pt on the photocatalytic properties of TiO_2 NWs as shown in Figure 6. It is obvious that MB degradated only a little in the absence of photocatalysts. For the Pt-TiO_2 NWs, the photodegradation efficiency of samples

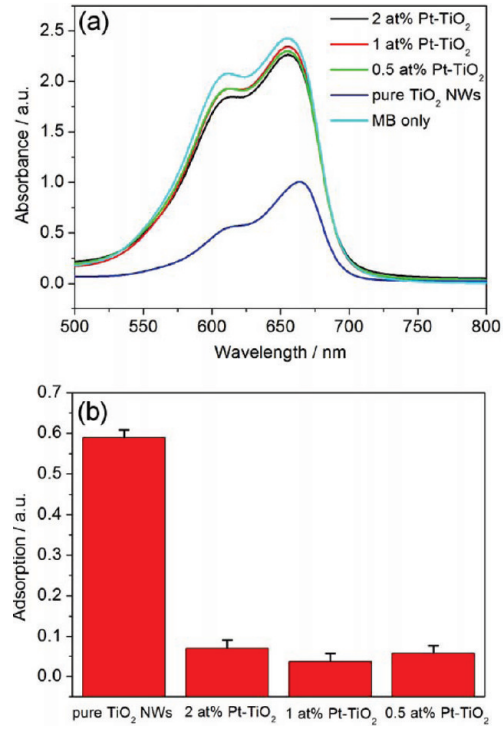

FIGURE 7. (a) Absorption spectra of left MB solutions after adsorption by photocatalysts for 48 h, (b) adsorption histogram of different materials.

is 1 at% Pt-TiO_2 > 0.5 at % Pt-TiO_2 > 2 at % Pt-TiO_2. It suggests that high Pt loading value does not mean high photocatalytic efficiency for the Pt-TiO_2 NWs hybrids. However, pure TiO_2 NWs seems more efficient than those modified by Pt nanoparticles as shown in Figure 6e. At the initial stages, the degradation efficiency of pure TiO_2 NWs is abnormally high compared with that of other photocatalysts. In fact, an adsorption process happened when the photocatalyst was added into the MB solution. The photocatalyst was stained blue obviously. The abnormally high degradation efficiency of pure TiO_2 NWs may be due to its excellent adsorption properties.

Further investigation about the adsorption properties of different materials was carried out. The photocatalysts were added into 20 mg/L of MB solutions. The solutions were stirred for 2 h and then stayed for 48 h in a dark room. Figure 7a shows absorption spectra of left MB solutions after the photocatalysts were centrifuged. It is obvious that the adsorption ability of pure TiO_2 NWs is much larger than modified ones. Figure 7b shows the corresponding adsorption histogram of different materials. The adsorption amounts are 58, 7, 4, and 6% for samples pure TiO_2 NWs, 2 at % Pt-TiO_2, 1 at % Pt-TiO_2, and 0.5 at % Pt-TiO_2, respectively. Another noteworthy phenomenon is that the Pt-TiO_2 NWs composites adsorb less MB than pure TiO_2 NWs. This suggests that Pt nanoparticles occupy the adsorption sites of MB. Moreover, the surface of Pt nanoparticles is not covered by MB.

The influence of adsorption on the photocatalytic properties was also investigated. Figure 8 shows the time-dependent photodegradation of MB under the illumination of UV light. The photocatalysts were used after adsorption of MB

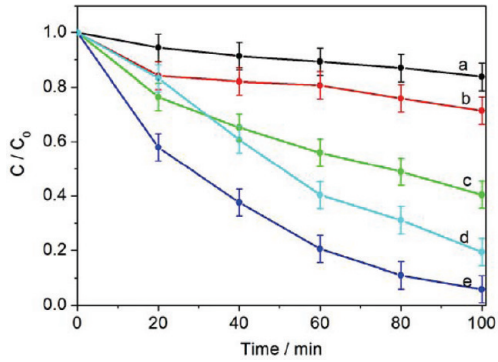

FIGURE 8. Time-dependent photodegradation of MB (20 mg/L, 50 mL) under the illumination of UV light (a) without photocatalysts, (b) pure TiO_2 NWs, (c) 2 at% Pt-TiO_2, (d) 0.5 at% Pt-TiO_2 and (e) 1 at% Pt-TiO_2. All the photocatalysts were used with adsorption of MB for 48 h in a dark room.

for 48 h in a dark room. Compared with the data in Figure 6, the photocatalytic ability of pure TiO_2 NWs was obviously weakened. There were more than 70% MB left for 100 min. It is believed that the abnormally high drop of MB concentration of pure TiO_2 NWs in Figure 6 is due to its excellent adsorption properties, not its photocatalytic activity.

High adsorption does not help to enhance the photocatalytic ability of pure TiO_2 NWs. However, the modification of Pt nanoparticles enhanced the photocatalytic properties of TiO_2 NWs obviously. There may be two reasons for this phenomenon. A Schottky barrier forms between TiO_2 and Pt naonoparticles, leading to a fast transport of photogenerated electrons to Pt particles (18, 19). This would decrease the electron−hole recombination. Furthermore, Pt on TiO_2 surface can accelerate the transfer of electrons to dissolved oxygen molecules (20). Pt modification was also reported to depress photocorrosion and this was helpful to improve the photocatalytic activity further (19). It is also observed that 1 at % Pt-TiO_2 sample has the highest photocatalytic efficiency among the three modified ones, as shown in Figures 6 and 8. It indicates that there is an optimum loading value, above which it can not help to enhance the photocatalytic ability of TiO_2 NWs. Of course, the optimum value would have a great relationship with the dispersion and particle sizes of Pt nanoparticles. It is considered that Pt particles, with high loading values, attract holes subsequently recombine them with electrons, served as recombination centers (21). Furthermore, Figure 8 shows that 2 at % Pt-TiO_2 sample has the highest light adsorption among all samples. However, it has the lowest photocatalytic efficiency. It indicates that the adsorption of light by Pt nanoparticles does not help to enhance the photocatalytic ability of TiO_2 NWs. Higher Pt loading values can absorb more incident photons which would not contribute to the photocatalytic efficiency.

Figure 9 shows evolution of the absorption spectrum of MB at different degradation time using 1 at % Pt-TiO_2 sample as the photocatalyst. The spectral peak wavelength gradually shifts to the blue region, from 655 nm at the initial time to 613 nm after 100 min, during the course of the photodegradation. This suggests that MB was *N*-demethylated in a stepwise manner in the degradation of MB (22).

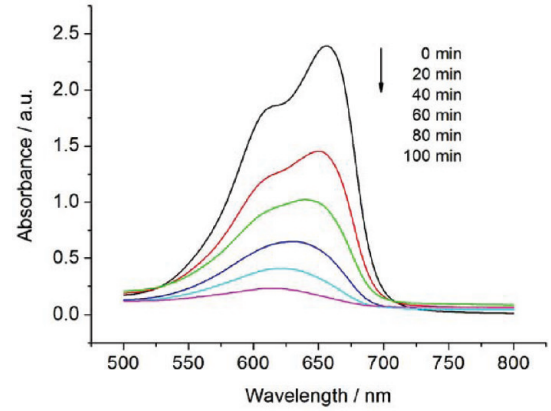

FIGURE 9. Evolution of the absorption spectrum of MB at different degradation time with 1 at% Pt-TiO_2 sample as photocatalyst. The photocatalysts were used with adsorption of MB for 48 h in a dark room.

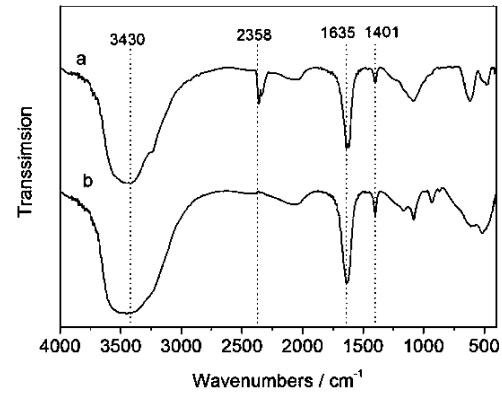

FIGURE 10. The FT-IR spectrum of samples (a) 1 at % Pt-TiO_2 and (b) pure TiO_2 NWs after the photodegradation of MB.

Methyl groups were removed one at a time as confirmed by the peak wavelength that gradually shifts toward the blue region.

Figure 10 shows the FT-IR spectra of samples after photodegradation of MB. The broad absorption peak appearing near 3400 cm^{-1} corresponds to stretching vibrational aspect of Ti−OH bands. The band around 1625 cm^{-1} was the characteristic peak of the bending vibrations of H−O−H. These two −OH groups are important to the photocatalytic reaction. The band centered at 1401 cm^{-1} is assigned to bending vibrations of C−H bond in the species linking −Ti−O-Ti- structural network (23, 24). The band around 2358 cm^{-1} is the stretching vibrational peak of CO_2. The peaks between 700 and 500 nm, correspond to the stretching bending vibrations of TiO_2. The peak around 500 cm^{-1} is due to stretching vibration of Ti−O−Ti around and the one around 600 cm^{-1} is due to bending vibration band of Ti−O and O−Ti−O. The C−H at 1401 cm^{-1} is possible from the shedding $-CH_3$ adsorbing on the surface of TiO_2 and Pt. The bending vibration of C−H bond of 1 at % Pt-TiO_2 sample is weaker than that of pure TiO_2 NWs. At the same time, the stretching vibrational peak of CO_2 of the former is much higher than that of the latter. The catalytic effect of Pt particles may be responsible for this phenomenon. It is well-known that Pt is efficient in the dehydroge-

nation. It is considered that the $-CH_3$ adsorbed on TiO_2 surface can be oxidized to CO_2 efficiently under the catalytic effect of Pt.

CONCLUSIONS

TiO_2 NWs with a diameter of 100−200 nm were prepared by a simple hydrothermal method. Pt nanoparticles with the average size of about 5 nm were uniformly deposited on the surface of TiO_2 NWs by a chemical reduction method. The photodegradation of MB under UV light indicated that Pt nanoparticles could enhance the photocatalytic effect of TiO_2 NWs obviously. However, there is an optimum Pt loading value, above which it can not help to enhance the photocatalytic ability of TiO_2 NWs by increasing the loading value. In our case, the 1 at% Pt-TiO_2 sample has higher photocatalytic activity than the other two samples, 2 at% Pt-TiO_2, 0.5 at% Pt-TiO_2 respectively. Besides enhancing the electron−hole separation and charge transfer to dissolved oxygen, Pt may also serve as an effective catalyst in the oxidation of MB from the FTIR result. The shedding $-CH_3$ can be oxidized to CO_2 efficiently under the catalytic effect of Pt.

Acknowledgment. We acknowledge support from the National Nature Science Foundation of China (50872071 and 50972079), the Shandong Natural Science Fund for Distinguished Young Scholars (JQ200915), Nature Science Foundation of Shandong Province (Y2007F03 and Y2008F26), Foundation of Outstanding Young Scientists in Shandong Province (No. 2006BS04030), Tai Shan Scholar Foundation of Shandong Province, and Gong Guan Foundation of Shandong Province (2008GG10003019).

REFERENCES AND NOTES

(1) Pucher, P.; Benmami, M.; Azouani, R.; Krammer, G.; Chhor, K.; Bocquet, J. F.; Kanaev, A. V. *Appl. Catal., A* **2007**, *332*, 297–303.
(2) Naya, S.; Inoue, A.; Tada, H. *J. Am. Chem. Soc.* **2010**, *132*, 6292–6293.
(3) Yang, D. J.; Liu, H. W.; Zheng, Z. F.; Yuan, Y.; Zhao, J. C.; Waclawik, E. R.; Ke, X. B.; Zhu, H. Y. *J. Am. Chem. Soc.* **2009**, *131*, 17885–17893.
(4) Denny, F.; Scott, J.; Chiang, K.; Teoh, W. Y.; Amal, R. *J. Mol. Catal. A: Chem.* **2007**, *263*, 93–102.
(5) Sun, B.; Vorontsov, A. V.; Smirniotis, P. G. *Langmuir* **2003**, *19*, 3151–3156.
(6) Kasuga, T.; Hiramatsu, M.; Hoson, A.; Sekino, T.; Niihara, K. *Adv. Mater.* **1999**, *11*, 1307–1311.
(7) Miao, Z.; Xu, D. S.; Ouyang, J. H.; Guo, G. L.; Zhao, X. S.; Tang, Y. Q. *Nano Lett.* **2002**, *2*, 717–720.
(8) Huang, J.; Cao, Y.; Huang, Q.; He, H.; Liu, Y.; Guo, W.; Hong, M. *Cryst. Growth Des.* **2009**, *9*, 3632–3637.
(9) Wang, P.; Zakeeruddin, S. M.; Comte, P.; Charvet, R.; Humphry-Baker, R.; Gr, M. *J. Phys. Chem. B* **2003**, *107*, 14336–14341.
(10) Burnside, S. D.; Shklover, V.; Barbe, C.; Comte, P.; Arendse, F.; Brooks, K.; Gratzel, M. *Chem. Mater.* **1998**, *10*, 2419–2425.
(11) Varghese, O. K.; Gong, D. W.; Paulose, M.; Ong, K. G.; Dickey, E. C.; Grimes, C. A. *Adv. Mater.* **2003**, *15*, 624–627.
(12) Fox, M. A.; Dulay, M. T. *Chem. Rev.* **1993**, *93*, 341–357.
(13) Hoffmann, M. R.; Martin, S. T.; Choi, W.; Bahnemann, D. W. *Chem. Rev.* **1995**, *95*, 69–96.
(14) Emilio, C. A.; Litter, M. I.; Kunst, M.; Bouchard, M.; Colbeau-Justin, C. *Langmuir* **2006**, *22*, 3606–3613.
(15) Hidalgo, M. C.; Maicu, M.; Navío, J. A.; Colón, G. *Catal. Today* **2007**, *129*, 43–49.
(16) He, Z. Q.; Xie, L.; Tu, J. J.; Song, S.; Liu, W. P.; Liu, Z. W.; Fan, J. Q.; Liu, Q.; Chen, J. M. *J. Phys. Chem. C* **2010**, *114*, 526–532.
(17) Vorontsov, A. V.; Savinov, E. N.; Jin, Z. S. *J. Photochem. Photobiol., A* **1999**, *125*, 113–117.
(18) Linsebigler, A. L.; Lu, G.; Yates, J. T. *Chem. Rev.* **1995**, *95*, 735–758.
(19) Zeng, H. B.; Cai, W. P.; Liu, P. S.; Xu, X. X.; Zhou, H. J.; Klingshirn, C.; Kalt, H. *ACS nano* **2008**, *2*, 1661–1670.
(20) Carp, O.; Huisman, C. L.; Reller, A. *Prog. Solid State Chem.* **2004**, *32*, 33–177.
(21) Wei, M.; Herrmann, J.; Pichat, P. *Catal. Lett.* **1989**, *3*, 73–84.
(22) Zhang, T. Y.; Oyama, T.; Aoshima, A.; Hidaka, H.; Zhao, J. C.; Serpone, N. *J. Photochem. Photobiol., A* **2001**, *140*, 163–172.
(23) Wang, J. A.; Limas-Ballesteros, R.; Lopez, T.; Moreno, A.; Gomez, R.; Novaro, O.; Bokhimi, X. *J. Phys. Chem. B* **2001**, *105*, 9692–9698.
(24) Chen, K.; Li, J. Y.; Li, J.; Zhang, Y. M.; Wang, W. X. *Colloids Surf., A* **2010**, *360*, 47–56.

AM100834X